Thermal equation of state of TiC: A synchrotron x-ray diffraction study

Xiaohui Yu,[1,2,3,a)] Zhijun Lin,[1] Jianzhong Zhang,[1] Liping Wang,[4] Zejun Ding,[3] Changqing Jin,[2] and Yusheng Zhao[1,a)]
[1]*LANSCE Division, Los Alamos National Laboratory, Los Alamos, New Mexico 87545, USA*
[2]*National Lab for Condensed Matter Physics, Institute of Physics, CAS, Beijing 100080, China*
[3]*Department of Physics, University of Science and Technology of China, Hefei 230026, China*
[4]*Mineral Physics Institute, State University of New York, Stony Brook, New York 11794, USA*

(Received 1 February 2010; accepted 27 April 2010; published online 3 June 2010)

The pressure–volume–temperature measurements were carried out for titanium carbide (TiC) at pressures and temperatures up to 8.1 GPa and 1273 K using energy-dispersive synchrotron x-ray diffraction. Thermoelastic parameters were derived for TiC based on a modified high-temperature Birch–Murnaghan equation of state and a thermal pressure approach. With the pressure derivative of the bulk modulus, K_0', fixed at 4.0, we obtain: the ambient bulk modulus $K_0=268(6)$ GPa, which is comparable to previously reported value; temperature derivative of bulk modulus at constant pressure $(\partial K_T/\partial T)_P=-0.026(9)$ GPa K^{-1}, volumetric thermal expansivity $\alpha_T(K^{-1})=a+bT$ with $a=1.62(12)\times10^{-5}$ K^{-1} and $b=1.07(17)\times10^{-8}$ K^{-2}, pressure derivative of thermal expansion $(\partial\alpha/\partial P)_T=(-3.62\pm1.14)\times10^{-7}$ GPa^{-1} K^{-1}, and temperature derivative of bulk modulus at constant volume $(\partial K_T/\partial T)_V=-0.015(8)$ GPa K^{-1}. These results provide fundamental thermophysical properties for TiC for the first time and are important to theoretical and computational modeling of transition metal carbides. © *2010 American Institute of Physics*. [doi:10.1063/1.3436571]

Titanium carbide (TiC) is a hard refractory metallic material of great scientific and technological interest. It possesses not only an extremely high melting point (3067 °C) but also excellent thermal and electrical conductivity and resistance to oxidation and corrosion.[1,2] Because of these characteristics, TiC finds broad and significant applications in industrial machinery, wear-resistant coating, and composite materials reinforcement. TiC, for example, can be infused to diamond under high-pressure and high-temperature conditions, resulting in a diamond composite of high electron density and super hardness.[3–5] At ambient conditions, TiC crystallizes in a rock-salt structure with a space group of $Fm3m$. In perfect and pure TiC, bonding is a complex mixture of covalent, ionic, and metallic types. The covalent component is attributed to the interactions between Ti $3d$ and C $2p$ states and is primarily responsible for the large values of the elastic constants of TiC and its high Debye temperature.

Thermal expansion and equation of state (EOS) are fundamental properties of condensed matter. These properties are often used to provide crucial tests for lattice-dynamical models and schemes utilized in electronic structure calculations and to model high-pressure–temperature ($P-T$) phenomena under dynamic shocks.[6,7] Although the EOS of TiC was recently studied at room temperature using synchrotron x-ray diffraction in a diamond anvil cell, the thermoelastic EOS of TiC has, to date, not been determined. The term "thermoelastic" emphasizes that the final outcomes of the EOS determination are thermoelastic properties of the matter, such as temperature derivative of bulk modulus and pressure derivative of thermal expansion. In this work, we performed pressure–volume–temperature ($P-V-T$) measurements on TiC in the temperature range 300–1273 K and at pressures up to 8.1 GPa. The experimental results allow us to derive a comprehensive EOS for the determination of thermoelastic properties of TiC.

In situ x-ray diffraction experiment was performed using a cubic-anvil apparatus installed on beamline X17B2 of the National Synchrotron Light Source, Brookhaven National Laboratory. The white radiation from the superconducting wiggler magnet was used for energy-dispersive measurements. The diffracted x-rays were collected with a multielement detector at a fixed Bragg angle of $2\theta=6.69°$. The cell assembly used in the present experiment is identical to the one described in Ref. 8. Briefly, a cube made up of a mixture of amorphous boron and epoxy resin was employed as pressure-transmitting medium and amorphous carbon was used as furnace material to achieve high temperatures. The TiC sample (Alfa, purity > 99.5%, with an average grain size of 2 μ, and an initial density of 4.93 g/cm^3), sandwiched by NaCl powder, was packed into a cylindrical container of boron nitride, 1.0 mm inner diameter and 2.0 mm length.

In the present study, NaCl was used as an internal pressure marker and the sample pressure was calculated from Decker's EOS for NaCl.[9] At each experimental condition, five NaCl diffraction peaks, 111, 200, 220, 222, and 420, were usually used for the determination of pressure. Within the accuracy of the Decker scale for NaCl, the uncertainty in pressure measurements is mainly due to the statistical variation in the positions of different diffraction peaks and is less than 0.1 GPa in the $P-T$ range investigated here. Temperatures were measured by a W/Re25%–W/Re3% thermocouple that was in direct contact with the sample. Temperature gradients over the entire sample container length (2 mm) were

a)Authors to whom correspondence should be addressed. Electronic addresses: xiaohui@lanl.gov and yzhao@lanl.gov.

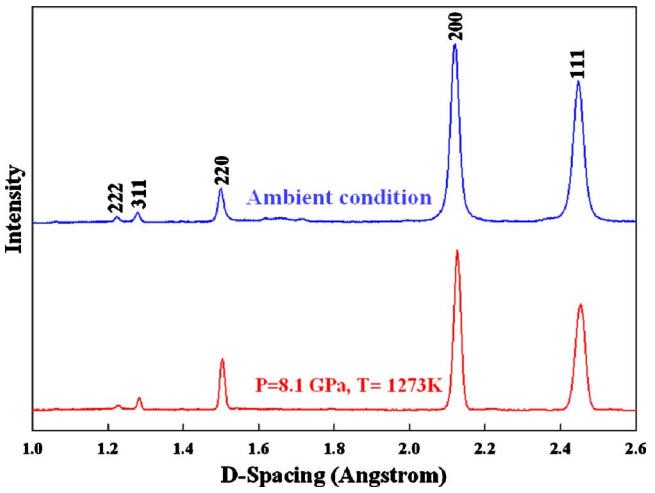

FIG. 1. (Color online) Representative x-ray diffraction patterns used for the refinement of unit-cell parameters of TiC under high $P-T$ conditions.

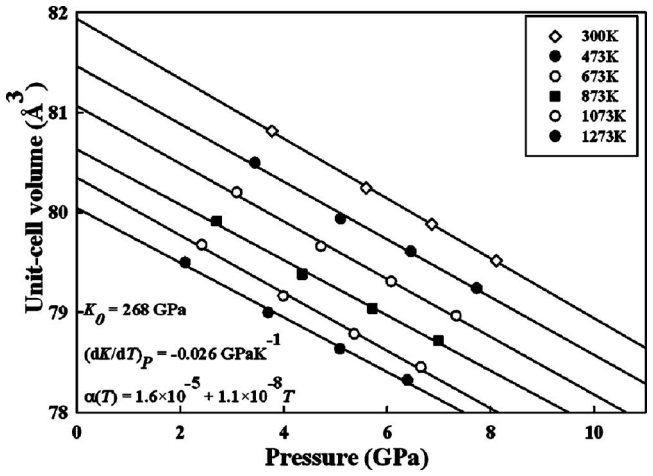

FIG. 2. $P-V-T$ data measured for TiC. The curves represent results of the least-squares fitting using Eq. (1).

on the order of 20 at 1500 K, and the radial temperature variations were less than 5 K at this condition.[8] Because x-ray diffraction patterns were obtained for both samples and NaCl in close proximity to the thermocouple junction, errors in temperature measurement were estimated to be around 10 K. No correction was applied for the effect of pressure on the thermocouple emf.

The experiment reported here was carried out by the following procedures. We first compressed the sample at room temperature to 9 GPa, followed by heating to the maximum temperature of 1273 K. Except for the first heating cycle, x-ray diffraction data for both TiC and NaCl were collected on cooling (1273, 1073, 873, 673, 473, and 300 K, with a counting time of ~1 min for each diffraction pattern) to minimize nonhydrostatic stress built-up during the room temperature compression. The same procedure was repeated several times at progressively lower pressures to obtain sufficient data at many different $P-T$ conditions and to yield a tight constraint on the zero pressure volumes. At the end of the experiment, the TiC sample was recovered with its initial lattice parameter within errors of the refinements (<0.1%), indicating no change in bulk composition or in system calibration over the entire experimental $P-T$ range. Examples of x-ray diffraction patterns at selected conditions are shown in Fig. 1; no phase transition was observed in the experimental $P-T$ range.

Peak positions were determined by the Gaussian peak fitting of diffracted intensity. The lattice parameters were calculated by least-squares fitting based on a cubic unit-cell, using diffraction lines of 111, 200, 220, 311, and 222. The uncertainties in the lattice parameter and unit-cell volume determination are within 0.1% of the parameter values. Figure 2 shows the relationship between the unit-cell volumes and pressures at several different temperatures.

We employ a modified high-T Birch–Murnaghan EOS,[10–15] truncated to third order, to derive thermoelastic parameters based on the measured $P-V-T$ data for TiC. A general form of this modified EOS is formulated by

$$P = 3K_T f(1+2f)^{5/2}\left[1 - \frac{3}{2}(4-K')f + \ldots\right], \quad (1)$$

where

$$K_T = K_{T0} + (\partial K/\partial T)_P(T-300),$$

$$K' = (\partial K/\partial P)_T,$$

and

$$f = \frac{1}{2}[(V_T/V_{PT})^{2/3} - 1],$$

$$V_T = V_0 \exp\left[\int \alpha(0,T)dT\right].$$

In Eq. (1), K_{T0} and K_T represent the isothermal bulk modulus at 300 K and a higher temperature T, and $(\partial K/\partial T)_P$ and $(\partial K/\partial P)_T$ stand for the temperature and pressure derivatives of the bulk modulus, respectively. V_0, V_T, and V_{PT} correspond to the unit-cell volumes at ambient conditions, at ambient pressure and temperature T, and at high $P-T$ conditions, respectively. $\alpha(0,T)$ is the volumetric thermal expansion at atmospheric pressure, commonly represented by $\alpha(0,T)=a+bT-c/T^2$ (T in Kelvin).[16] In the modified high-T Birch–Murnaghan EOS, the temperature effects were taken into account by replacing K_0 with K_T and substituting V_0/V_P with V_T/V_{PT} in the isothermal EOS. Because of the limited pressure coverage that restricts an accurate constraint on K' for TiC, we assume $K'=4$ in Eq. (1) throughout the data analysis. Similarly, we ignore the term of c/T^2 in $\alpha(0,T)$ as well as higher-order terms and cross derivatives of the bulk modulus such as ∂^2K/∂^2T and $\partial^2K/\partial P\partial T$. From a least-squares fit to all $P-V-T$ data using Eq. (1), we obtain $K_0=268(6)$ GPa, $(\partial K/\partial T)_P=-0.026(9)$ GPa K^{-1}, and $\alpha(0,T)=a+bT$ with $a=1.62(12)\times10^{-5}$ K^{-1} and $b=1.07(17)\times10^{-8}$ K^{-2}. Errors of thermoelastic parameters in the present study are those of the least-squares fitting. Uncertainties in the $P-V-T$ measurements were not included in the error estimation. The K' has been much better constrained from a recent static compression experiment in a

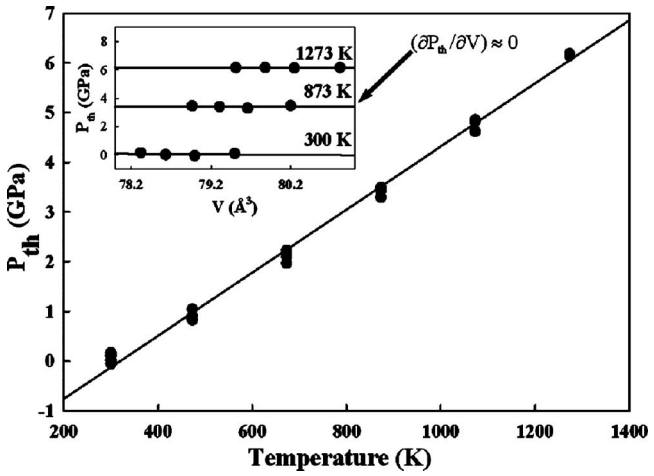

FIG. 3. Thermal pressure (P_{th}) of TiC as a function of temperature. The spread of the data points at any given temperature corresponding to thermal pressures at different volumes, which is plotted in detail in the inset. The lines in the inset plot show approximate constant values of thermal pressure for a given temperature.

diamond anvil cell[17] and is reported to be 4.8. Using this K', we obtain $K_0=265(6)$ GPa and $(\partial K/\partial T)_P=-0.024(9)$ GPa K^{-1}; $a=1.62(12)\times10^{-5}$ K^{-1} and $b=1.08(17)\times10^{-8}$ K^{-2}. For both analyses, the resultant bulk moduli at room temperature are comparable to those reported in Ref. 17 ($K_0=268(2)$ GPa with K' fixed at 4 and $K_0=254(7)$ GPa for $K'=4.8$). In addition, the volumetric thermal expansion obtained from the present work at 300 K (1.94×10^{-5} K^{-1}) is in excellent agreement with that reported in Ref. 18 (1.96×10^{-5} K^{-1}).

From the thermodynamic identity,

$$(\partial\alpha/\partial P)_T=(\partial K/\partial T)_P K_{T0}^{-2}, \tag{2}$$

the pressure derivative of the volume thermal expansivity, $(\partial\alpha/\partial P)_T$, is found to be $-3.62\pm1.44\times10^{-7}$ K^{-1} GPa^{-1}. The uncertainty in $(\partial\alpha/\partial P)_T$ is estimated from the error propagation of K_{T0} and $(\partial K/\partial T)_P$.

The thermal-pressure approach to process $P-V-T$ data has been widely applied for its thermodynamic importance.[14,19–22]This method is also useful for deriving thermoelastic parameter $(\partial K_T/\partial T)_V$, the temperature derivative of bulk modulus at constant volume, which is experimentally difficult to measure. In this approach, thermal pressure P_{th} is calculated as the difference between the measured pressure at a given temperature and the calculated pressure from Eq. (1) at room temperature, with both pressures corresponding to the same volume. Following this definition, thermal pressures were calculated for TiC and are plotted in Fig. 3. An inspection of Fig. 3 demonstrates that thermal pressure varies linearly with temperature, which is consistent with the linear trend revealed in many different classes of condensed matter.[14–16,19–22] Thermal pressure at any temperature above 300 K for a given volume can also be analyzed from thermodynamic relations. Following the method of Anderson[16,19] and his subsequent studies, thermal pressure was calculated by

$$P_{th}=\int_{300}^{T}\left(\frac{\partial P}{\partial T}\right)_V dT=P_{th}(V,T)-P_{th}(V,300)$$
$$=[\alpha K_T(V_{300},T)+(\partial K_T/\partial T)_V\ln(V_{300}/V)](T-300). \tag{3}$$

From the least-squares fit of the thermal pressure versus temperature shown in Fig. 3, we obtain average values of $\alpha K_T(V_{300},T)$ and $(\partial K_T/\partial T)_v$ that are 0.0061(1) GPa K^{-1} and $-0.015(8)$ GPa K^{-1}, respectively. From the thermodynamic identity,

$$(\partial K_T/\partial T)_V=(\partial K_T/\partial T)_P+(\partial K_T/\partial P)_T\alpha K_T(V_{300},T). \tag{4}$$

We obtain a value of $-0.040(20)$ for $(\partial K_T/\partial T)_P$, which within the uncertainties of the fittings, is in agreement with the results derived from Eq. (1). The value of $(\partial\alpha/\partial P)_T$ derived from Eq. (2) is $(-5.57\pm2.79)\times10^{-7}$ K^{-1} GPa^{-1}. Internally consistent thermal EOSs for TiC, as summarized in Table I, are thus obtained using different analysis methods. Within the experimental uncertainties, the K_0 value we obtained is comparable to those of previous studies (see Table I), whereas the thermoelastic parameters $(\partial K_T/\partial T)_P$, $(\partial K_T/\partial T)_V$, and $(\partial\alpha/\partial P)_T$ for TiC are determined for the first time for TiC.

In summary, we have conducted *in situ* high-pressure diffraction experiments on TiC at pressures up to 8.1 GPa and temperatures up to 1273 K. Two different methods, namely, high-T EOS and thermal pressure, have been applied in the data analysis. From these measurements, we have derived a complete thermal EOS for TiC, which includes temperature and pressure derivatives of thermal expansion and elastic bulk modulus. Within the experimental uncertainty, the bulk modulus obtained in our study is in good agreement with the value determined with diamond anvil cell.[17] These

TABLE I. Summary of thermoelastic parameters for TiC. Except for $(\partial\alpha/\partial P)_T$, the numbers in parentheses are standard deviations from the least-squares fits and refer to the last digit(s) of the parameter values. For $(\partial\alpha/\partial P)_T$, the uncertainties are estimated from the error propagation of K_0 and $(\partial K/\partial T)_P$.

Reference	K_0 (GPa)	K_0'	$(\partial K/\partial T)_P$ (GPa K^{-1})	$\alpha_T(\mathrm{K}^{-1})=a+bT$ $a,10^{-5}$	$b,10^{-8}$	$(\partial\alpha/\partial P)_T$ (10^{-7} GPa^{-1} K^{-1})	$(\partial K_T/\partial T)_V$ (GPa K^{-1})
This work[a]	268(6)	4	−0.026(9)	1.62(12)	1.07(17)	−3.62 ± 1.14	
This work[b]	268(6)	4	−0.040(20)			−5.57 ± 2.79	−0.015(8)
17	268(2)	4					
17	254(7)	4.8					

[a]Based on the measured $P-V-T$ data and Eqs. (1) and (2).
[b]Thermal-pressure approach based on the measured data and Eqs. (3) and (4).

results extend our knowledge of the fundamental thermo physical properties on TiC and are important to theoretical and computational modeling of transition metal carbides.

ACKNOWLEDGMENTS

This research was supported by Los Alamos National Laboratory, which is operated by Los Alamos National Security LLC under DOE Contract No. DEAC52-06NA25396. The experimental work was carried out at beam line X17B2 of the National Synchrotron Light Source, Brookhaven National Laboratory, which is supported by the Consortium for Materials Properties Research in Earth Sciences (COMPRES) under NSF cooperative agreement (Contract No. EAR 01-35554).

[1]Y. Shin, X. S. Li, C. Wang, J. R. Coleman, and G. J. Exarhos, Adv. Mater. (Weinheim, Ger.) **16**, 1212 (2004).
[2]D. Strzeciwilk, Z. Wokulski, and P. Tracz, J. Alloys Compd. **350**, 256 (2003).
[3]Y. Zhao, J. Qian, L. L. Daemen, C. Pantea, J. Zhang, G. A. Voronin, and T. W. Zerda, Appl. Phys. Lett. **84**, 1356 (2004).
[4]T. Yu, Y. Deng, L. Wang, R. Liu, and L. Zhang, Adv. Mater. (Weinheim, Ger.) **19**, 2301 (2007).
[5]P. Zhu, Y. Hong, B. Liu, and G. Zou, Nanotechnology **20**, 255603 (2009).
[6]D. C. Wallace, Los Alamos Scientific Laboratory Report No. LA12020, January 1991.
[7]O. L. Anderson, *Equations of State of Solids for Geophysics and Ceramic Science* (Oxford University Press, Oxford, 1995).
[8]D. J. Weidner, M. T. Vaughan, J. Ko, Y. Wang, X. Liu, R. E. Pacalo, and Y. Zhao, in *High-Pressure Research: Application to Earth and Planetary Sciences*, edited by Y. Syono and M. H. Manghnani (American Geophysics Union, Washington, DC, 1992), p. 13.
[9]D. L. Decker, J. Appl. Phys. **42**, 3239 (1971).
[10]F. D. Murnaghan, Am. J. Math. **59**, 235 (1937).
[11]F. Birch, Phys. Rev. **71**, 809 (1947).
[12]S. K. Saxena and J. Zhang, Phys. Chem. Miner. **17**, 45 (1990).
[13]Y. Zhao, D. Schiferl, and T. J. Shankland, Phys. Chem. Miner. **22**, 393 (1995).
[14]Y. Zhao, A. C. Lawson, J. Zhang, B. I. Bennett, and R. B. Von Dreele, Phys. Rev. B **62**, 8766 (2000).
[15]Y. Wang, J. Zhang, H. Xu, Z. Lin, L. L. Daemen, Y. Zhao, and L. Wang, Appl. Phys. Lett. **94**, 071904 (2009).
[16]I. Suzuki, J. Phys. Earth **23**, 145 (1975).
[17]Q. Gu, G. Krauss, F. Gramm, and W. Steurer, J. Phys.: Condens. Matter **20**, 445226 (2008).
[18]J. F. Shackelford and W. Alexander, *CRC Materials Science and Engineering Handbook* (CRC Press, Boca Raton, FL, 2001), p. 451.
[19]O. L. Anderson, J. Geodyn. **1**, 185 (1984).
[20]J. Zhang and F. Guyot, Phys. Chem. Miner. **26**, 206 (1999).
[21]J. Zhang and P. Kostak, Phys. Earth Planet. Inter. **129**, 301 (2002).
[22]J. Zhang, Y. Zhao, R. S. Hixson, G. T. Gray, L. Wang, W. Utsumi, S. Hiroyuki, and H. Takanori, Phys. Rev. B **78**, 054119 (2008).